

In the previous chapter we have seen that both constant dispersion and dispersion-managed solitons are important pulses in the study of long-distance transmission/communications. It is noteworthy that experiments reveal that solitons or localized pulses are also present in mode-locked (ML) lasers. Femtosecond solid-state lasers, such as those based on the Ti:sapphire (Ti:S) gain medium, and fiber ring lasers have received considerable attention in the field of ultra-fast science. In the past decade, following the discovery of mode-locking, the improved performance of these lasers has led to their widespread use, cf. Cundiff et al. (2008). In most cases interest in ultra-short pulse mode-locking has been in the net anomalous dispersive regime. But mode-locking has also been demonstrated in fiber lasers operating in the normal regime. Mode-locking operation has been achieved with relatively large pulse energies (Ilday et al., 2004b,a; Chong et al., 2008b).

In our investigations we have employed a distributive model, termed the power-energy saturation (PES) equation (cf. Ablowitz et al., 2008; Ablowitz and Horikis, 2008, 2009b; Ablowitz et al., 2009c). This model goes beyond the well-known master laser equation, cf. Haus (1975, 2000), in that it contains saturable power (intensity) terms; i.e., terms that saturate due to large field amplitudes. This equation has localized pulses that propagate and mode-lock in both an anomalous and a normally dispersive laser for both in the constant as well as dispersion-managed system. This is consistent with recent experimental observations (Ilday et al., 2004b; Chong et al., 2008a). We also note that it has been shown that dispersion-managed models with saturable power (intensity) energy saturation terms are in good agreement with experimental results in Ti:sapphire lasers (Sanders et al., 2009b). Pulse formation in an ultra-short pulse laser is typically dominated by the interplay between dispersion and nonlinearity. Suitable gain media and an effective saturable absorber are essential for initiating the mode-locking operation from intra-cavity background

fields and subsequent stabilization of the pulse. In the anomalous regime the mode-locked soliton solutions are found to approximately satisfy nonlinear Schrödinger (NLS)-type equations. The main difference between the NLS and PES equations, for both the constant and dispersion-managed cases, is that when gain and loss are introduced as in the PES equation, only one value of the propagation constant is allowed. Thus unlike the classical NLS equation there is not a full parameter family of solutions. In the normal dispersive regime the pulses are found to be significantly chirped and much broader, i.e., they are slowly varying, than those in the anomalous regime. These NLS equations with gain and loss terms are interesting and natural to study in the context of nonlinear waves.

In order to obtain localized or solitary waves, or as called in the physical literature, solitons, we often employ numerical methods. The numerical method, which we employed earlier in the study of communications (Ablowitz and Biondini, 1998; Ablowitz et al., 2000b), for numerically obtaining soliton solutions, is based upon taking the Fourier transform of the nonlinear equation, introducing a convergence factor, and then iterating the resulting equation until convergence to a fixed point in function space. The method was first introduced in 1976 (Petviashvili, 1976). The convergence factor depends on the homogeneity of the nonlinear terms. The technique works well for problems with a single polynomial nonlinear term (Pelinovsky and Stepanyants, 2004). However, many interesting systems are more complex. Recently, another way of finding localized waves was introduced (Ablowitz and Musslimani, 2005). The main ideas are to go to Fourier space (this part is the same as Petviashvili, 1976), then renormalize variables and obtain an algebraic system coupled to the nonlinear integral equation. We have found the method of coupling to be effective and straightforward to implement. The localized mode is determined from a convergent fixed point iteration scheme. The numerical technique is called spectral renormalization (SPRZ); it finds localized waves to a variety of nonlinear problems that arise in nonlinear optics and fluid dynamics. See also Chapter 10.

11.1 Mode-locked lasers

A laser is essentially an optical oscillator and as such it requires amplification, feedback and loss in its operation. The amplification is provided by stimulated emission in the gain medium. Feedback is provided by the laser “cavity”, which is often a set of mirrors that allow the light to reflect back on itself. One of the mirrors transmits a small fraction of the incident light to provide output.

The loss that counteracts gain is due to a variety of factors such as a field cutoff or polarization effects, etc.

A mode-locked pulse refers to the description of how ultra-short pulses are generated by a laser. The formation of a mode means that the electromagnetic field is essentially unchanged after one round trip in the laser. This implies that lasing occurs for those frequencies for which the cavity length is an integer number of wavelengths. If multiple modes lase at the same time, then a short pulse can be formed if the modes are also phase-locked; we say the laser is mode-locked, cf. Cundiff (2005). In terms of the mathematics of nonlinear waves, mode-locking usually relates to specific pulse solutions admitted by the underlying nonlinear equations.

A distinguishing feature of such a laser is the presence of an element in the cavity that causes it to mode-lock. This can be an active or a passive element. Passive mode-locking has produced shorter pulses and has a saturable absorber, i.e., one where the absorption saturates. In this case, higher intensity is less attenuated than a lower intensity.

An advantage of Ti:s lasers is their large-gain bandwidth, which is necessary for supporting ultra-short pulses (it is useful to think of this as the Fourier relationship). The gain band is typically quoted as extending from 700 to 1000 nm, although lasing can be achieved well beyond 1000 nm. The Ti:s crystal provides the essential mode-locking mechanism in these lasers. This is due to a strong cubic nonlinear index of refraction (the Kerr effect), which is manifested as an increase of the index of refraction as the optical intensity increases. Together with a correctly positioned effective aperture, the nonlinear Kerr-lens can act as a saturable absorber, i.e., high intensities are focused and hence transmit fully through the aperture while low intensities experience losses. Since short pulses produce higher peak powers, they experience a lower loss that also favors a mode-locked operation. This mode-locking mechanism has the advantage of being essentially instantaneous. However, it has the disadvantage of often being not self-starting; typically it requires a critical misalignment from optimum continuous wave operation. Ti:s lasers can produce pulses on the order of a few femtoseconds. An application of interest is producing a very long string of equally spaced mode-locked pulses: this has the potential to be used as an “optical clock” where each tick of the clock corresponds to a pulse, cf. Cundiff (2005). A schematic diagram of a typical Ti:s laser system is given in Figure 11.1 with typical units: pulsewidth: $\tau = 10 \text{ fs} = 10^{-14} \text{ s}$ and repetition time: $T_r = 10 \text{ ns} = 10^{-8} \text{ s}$ or repetition frequency $\text{fr} = \frac{1}{T_r} = 100 \text{ MHz}$. In this setup the prism pair is used to compensate for the net normal dispersion of the Ti:s crystal. In the crystal we have strong nonlinear effects, but in the prism the nonlinearity is very weak. So we assume

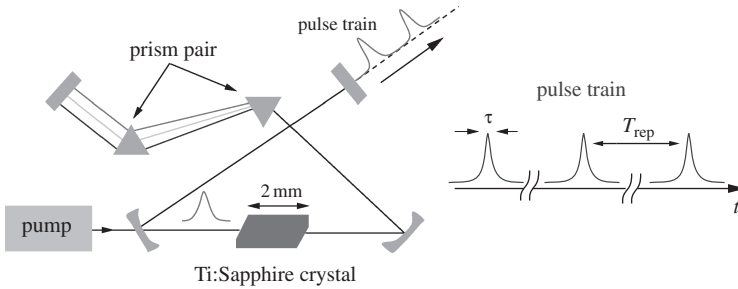


Figure 11.1 Left: Ti:sapphire laser; right: the pulse train.

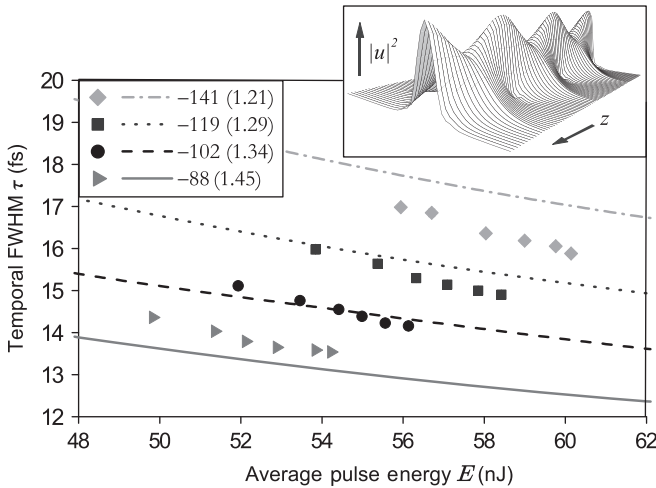


Figure 11.2 Curves are given from DMNLS theory. Symbols: experiments; inset: Dispersion-managed soliton.

a linear state in the prisms. This laser system is dispersion-managed and the nonlinearity is also varying along the laser cavity.

Quraishi et al. (2005) produced ultrashort pulses for a number of average net anomalous dispersions. The results were compared with theory based upon the dispersion-managed NLS equation (i.e., the DMNLS equation) discussed in the previous section. The results were favorable and are indicated in Figure 11.2. The different symbols correspond to different average dispersions times the cavity length: $\langle k''(z) \rangle l_m$. The graph and figures relate the pulsewidth τ to the energy of a pulse.

However the important feature of mode-locking is left out of the DMNLS theory. The DMNLS equation predicts a continuous curve for each average

dispersion value. But the experiments indicate that there is not a continuous curve, rather for each value of energy there is one mode-locked configuration. This is discussed next as part of the mathematical model.

11.2 Power-energy-saturation equation

The distributed model that we use to describe the propagation of pulses in a laser cavity is given in dimensionless form by

$$iu_z + \frac{d(z)}{2}u_{tt} + n(z)|u|^2u = \frac{ig}{1 + E/E_0}u + \frac{i\tau}{1 + E/E_0}u_{tt} - \frac{il}{1 + P/P_0}u, \quad (11.1)$$

where $d(z)$, $n(z)$ are the dispersion and coefficient of nonlinearity, each of which vary rapidly in z , $E(z) = \int_{-\infty}^{\infty} |u|^2 dt$ is the pulse energy, E_0 is related to the saturation energy, $P(z, t) = |u|^2$ is the instantaneous pulse power, P_0 is related to the saturation power, and the parameters g , τ , l , are all positive, real constants. The first term on the right-hand side represents saturable gain, the second is spectral filtering and the third saturable loss that reflects the fast saturable absorber: $\frac{l}{1+P/P_0}$.

Notice that gain and filtering are saturated with energy while loss is saturated with power. The gain and filtering mechanisms are related to the energy of the pulse while the loss is related to the power (intensity) of the pulse. Saturation terms can be expected to prevent the pulse from reaching a singular state; i.e., “infinite” energy or a blow-up in amplitude. Indeed, if blow-up were to occur that would suggest that both the amplitude and the energy of the pulse would become large, which in turn, make the perturbing effects small thus reducing the equation to the unperturbed NLS, which admits a stable, finite solution.

We refer to (11.1) as the power-energy-saturation equation or simply the PES equation. The right-hand side of (11.2) is what we will refer to as the perturbing contribution; it is denoted hereafter by $R[u]$.

The PES model reflects many developments over the years. In order to model the effects of nonlinearity, dispersion, bandwidth limited gain, energy saturation and intensity discrimination in a laser cavity the so-called master equation was introduced, cf. Haus et al. (1992); Haus (2000). The master equation is a generalization of the classical NLS equation, modified to contain gain, filtering and loss terms; the normalized master equation, with dispersion management included is given below.

$$iu_z + \frac{d(z)}{2}u_{tt} + n(z)|u|^2u = \frac{ig}{1 + E/E_0}u + \frac{i\tau}{1 + E/E_0}u_{tt} - i(l - \beta|u|^2)u.$$

The master equation is obtained from the PES model by Taylor expanding the power saturation term and putting $\beta = l/P_0$. As with the PES model, gain and filtering are saturated by energy (i.e., the time integral of the pulse power), but in the master equation the loss is converted into a linear and a cubic nonlinear term. For certain values of the parameters this equation exhibits a range of phenomena including: mode-locking evolution; pulses that disperse into radiation; some that evolve to a non-localized quasiperiodic state; and some whose amplitude grows rapidly (Kapitula et al., 2002). In the latter case, if the nonlinear gain is too high, the linear attenuation terms are unable to prevent the pulse from blowing up; i.e., the master mode-locking model breaks down (Kutz, 2006). However, unlike what is observed in experiments, there is only a small window of parameter space that allows for the generation of stable mode-locked pulses. In particular, the model is highly sensitive to the nonlinear loss/gain parameter.

We have shown that the PES model yields mode-locking for wide ranges of the parameters (cf. Ablowitz et al., 2008; Ablowitz and Horikis, 2008, 2009b; Ablowitz et al., 2009c). As mentioned above, this model is a distributed equation. There are also interesting lumped models that have been studied (cf. Ilday et al., 2004b,a; Chong et al., 2008b); e.g., in some laser models, loss is introduced in the form of fast saturable power absorbers that are placed periodically. It has been found (Ablowitz and Horikis, 2009a), however, that all features are essentially the same in both lumped and distributive models thus indicating that distributive models are very good descriptions of modes in mode-locked lasers. Lumped models reflect sharp changes in the parameters/coefficients due to corresponding elements in the system; mathematically these models are often dealt with by Dirac delta function transitions (see also Chapter 10). Mathematically it is also more convenient to work with distributed models. We note that Haus (1975) derived models of fast saturable absorbers in two-level media that are similar to the ones we are studying here. However in order to obtain analytical results, Haus Taylor-expanded and therefore obtained the cubic nonlinear model of a fast saturable absorber.

We also mention that to overcome the sensitivity inherent in the master equation, other types of terms, such as quintic terms, can be added to the master equation in order to stabilize the solutions. This increases the parameter range for mode-locking somewhat (instabilities may still occur); but it also adds another parameter to the model. Cubic and quintic nonlinear models are based on Ginzburg–Landau-type (GL) equations (cf. Akhmediev and Ankiewicz, 1997). In fact, if the pulse energy is taken to be constant the master equation reduces to a GL-type system. In general, GL-type

equations exhibit a wide spectrum of interesting phenomena and pulses that exhibit complex and chaotic dynamics and ones whose amplitude grows rapidly.

11.2.1 The anomalous dispersion regime

We first discuss the constant dispersive case in which case the laser cavity is described, in dimensionless form, by (called here the constant dispersion PES equation)

$$iu_z + \frac{d_0}{2}u_{tt} + |u|^2u = \frac{ig}{1 + E/E_0}u + \frac{i\tau}{1 + E/E_0}u_{tt} - \frac{il}{1 + P/P_0}u \quad (11.2)$$

with d_0 representing the constant dispersion, $n(z) = 1$, and remaining parameters defined above.

In what follows we keep all terms constant and only change the gain parameter g . More precisely, we take typical values: $E_0 = P_0 = 1$, $\tau = l = 0.1$, assume anomalous dispersion: $d_0 = 1$ ($d_0 > 0$), and in the evolution studies we take a unit Gaussian initial condition. For stable soliton solutions to exist the gain parameter g needs only to be sufficiently large to counter the two loss terms. It is also noted that we employ a fourth-order Runge–Kutta method to evolve (11.2) in z .

The evolution of the pulse peak for different values of the gain parameter g is shown in Figure 11.3. When $g = 0.1$ the pulse vanishes quickly due to excessive loss with no noticeable oscillatory behavior; the pulse simply decays, yielding damped evolution. When $g = 0.2, 0.3$, due to the loss in the system, the pulse initially undergoes a sharp decrease relative to its amplitude. However, it rapidly recovers and evolves into a stable solution. Much like the damped evolution, the amplitude is initially decreased but the resulting evolution is stable. Interestingly, e.g., when $g = 0.7, 1$, and the perturbations can no longer be considered small, a stable evolution is nevertheless again obtained, although somewhat different from the case above. Now with considerable gain in the system, the pulse amplitude increases rapidly and then a steady state is reached typically after some oscillations. The only major difference between the resulting modes is the resulting amplitude and the width of the pulse: i.e., for larger g the pulse is larger and narrower (Ablowitz and Horikis, 2008).

The above suggests that in the PES model, the mode-locking effect is generally present for $g \geq g^*$, a critical gain value. Without enough gain i.e., $g < g^*$, pulses dissipate to the trivial zero state. Furthermore, for this class of initial data and parameters studied, there are no complex radiation states or states

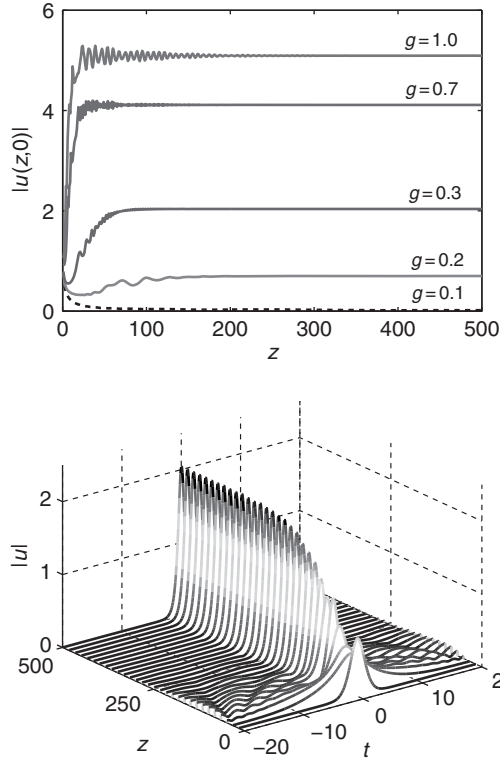


Figure 11.3 Evolution of the pulse peak, $|u(z, 0)|$, of an arbitrary initial profile under PES with different values of gain. The damped pulse-peak evolution is shown with a dashed line. In the bottom figure, a typical evolution is given for $g = 0.3$.

whose amplitudes grow without bound. In terms of solutions, (11.2) admits soliton states for all values of $g \geq g^* > l$ (recall, here $l = 0.1$). This can also be understood and confirmed by analytical methods (soliton perturbation theory) (Ablowitz et al., 2009a). Mode-locking of the solution is found to tend to soliton states. By a soliton state we mean a solution of the form $u(t, z) = f(t)\exp(-i\mu z)$, where μ is usually referred to as the propagation constant and $f(t)$ is the soliton shape.

As mentioned above, as the gain parameter increases so does the amplitude, and the pulse becomes narrower. In fact, it is observed that the energy changes according to $E \sim \sqrt{\mu}$. Indeed, from the soliton theory of the classical NLS equation this is exactly the way a classical soliton's energy changes, the key difference between the PES and pure NLS equation being that in

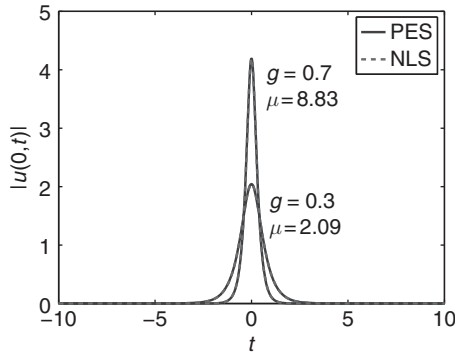


Figure 11.4 Solitons of the perturbed and unperturbed equations.

the pure NLS equation a semi-infinite set of μ exists, whereas now for the PES equation μ is unique for the given set of parameters. Once mode-locking occurs we find the solutions of the two equations, PES and NLS, are comparable. In Figure 11.4 we plot the two solutions for different values of g . In each case the same value of μ is used. The amplitudes match so closely that they are indistinguishable in the figure, meaning the perturbing effect is strictly the mode-locking mechanism, i.e., its effect is to mode-lock to a soliton of the pure NLS with the appropriate propagation constant. The solitons of the unperturbed NLS system are well known in closed analytical form, i.e., they are expressed in terms of the hyperbolic secant function, $u = \sqrt{2\mu} \operatorname{sech}(\sqrt{2\mu} t) \exp(-i\mu z)$, and therefore describe solitons of the PES to a good approximation.

Soliton strings

As mentioned above, solitons are obtained when the gain is above a certain critical value, $g > l$, otherwise pulses dissipate and eventually vanish (Ablowitz and Horikis, 2008). As gain becomes stronger, additional soliton states are possible and two, three, four or more coupled pulses are found to be supported; we call these states soliton strings. As above, we set $\tau = l = 0$, $E_0 = P_0 = d_0 = n = 1$ and vary the gain parameter g . The value of $\Delta\xi/\alpha$, where $\Delta\xi$ and α are the pulse separation and pulsewidth (the full width of half-maximum (FWHM) for pulsewidth is used) respectively, is a useful parameter. We measure $\Delta\xi$, between peak values of two neighboring pulses, and $\Delta\phi$ is the phase difference between the peak amplitudes. With sufficient gain ($g = 0.5$) equation (11.2) is evolved starting from unit Gaussians with initial peak separation $\Delta\xi = 10$ and $\Delta\xi/\alpha = 8.5$. The evolution and final state are depicted in Figure 11.5. For the

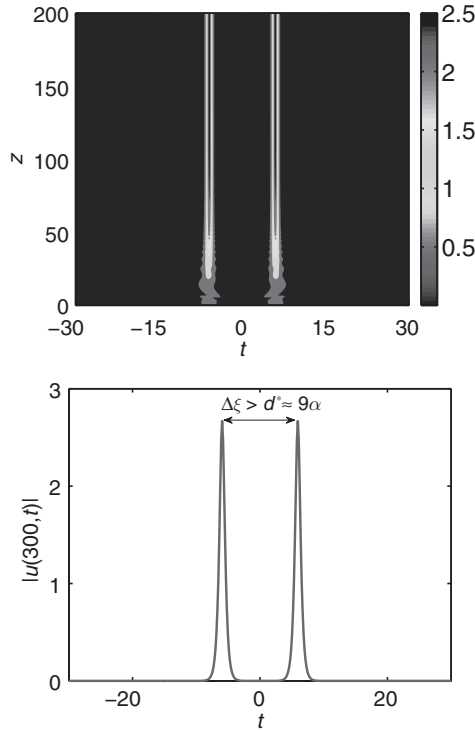


Figure 11.5 Top: Mode-locking evolution for an in phase two-soliton state of the anomalously constant dispersive PES equation; Bottom: the resulting soliton profile at $z = 300$. Here $g = 0.5$.

final state we find $\Delta\xi/\alpha \approx 10$. The resulting individual pulses are similar to the single soliton mode-locking case (Ablowitz and Horikis, 2008), i.e., individual pulses are approximately solutions of the unperturbed NLS equation, namely hyperbolic secants. We also note that the individual pulse energy is smaller than that observed for the single-soliton mode-locking case for the same choice of g , while the total energy of the two-soliton state is larger. This is due to the non-locality of energy saturation in the gain and filtering terms (Ablowitz et al., 2009c).

To investigate the minimum distance, d^* , between the solitons in order for no interactions to occur (in a prescribed distance) we evolve the equation starting with two solitons. If the initial two pulses are sufficiently far apart then the propagation evolves to a two-soliton state and the resulting pulses have a constant phase difference. If the distance between them is smaller than a critical value then the two pulses interact in a way characterized by the difference

in phase between the peaks amplitudes: $\Delta\phi$. When initial conditions are symmetric (in phase) two pulses are found to merge into a single soliton of (11.2). When the initial conditions are antisymmetric (out of phase by π) then they repel each other until their separation is larger than this critical distance while retaining the same difference in phase, resulting in an effective two-pulse high-order soliton state. The above situation is found with numerous individual pulses ($N = 2, 3, 4, \dots$). This situation does not occur in the pure NLS equation where two out-of-phase pulses strongly repel each other. The interaction phenomena can be described by perturbation theory (Ablowitz et al., 2009a). In the constant dispersion case this critical distance is found to be $\Delta\xi = d^* \approx 9\alpha$ (see Figure 11.5) where effectively no interaction occurs for $z < z_*$, corresponding to soliton initial conditions. Interestingly, this is consistent with the experimental observations of Tang et al. (2001). To further illustrate, we plot the evolution of in and out of phase cases in Figure 11.6. At $z = 500$ for the repelling solitons we find $\Delta\xi/\alpha = 8.9$.

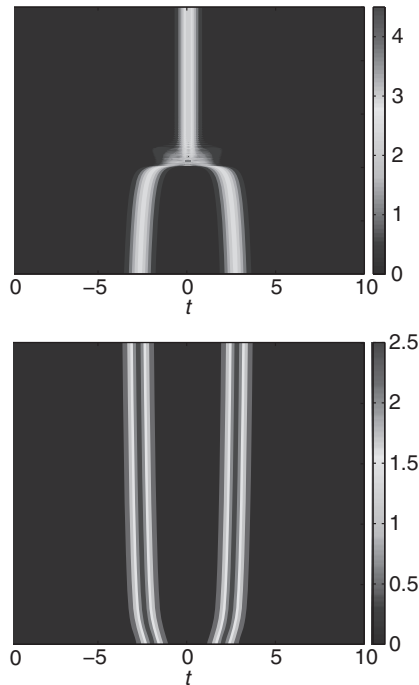


Figure 11.6 Two-pulse interaction when $\Delta\xi < d^*$. Initial pulses ($z = 0$) in phase: $\Delta\phi = 0$, $\Delta\xi/\alpha \approx 7$ (top) merge while those out of phase by $\Delta\phi = \pi$ with $\Delta\xi/\alpha \approx 6$ (bottom) repel. Here $g = 0.5$.

11.2.2 Dispersion-managed PES equation

Next we will discuss the situation when we employ the dispersion-managed PES equation (11.1). As in the communications application in the previous section, $d(z)$ is large and both $d(z)$ and $n(z)$ are rapidly varying. We take

$$d(z) = d_0 + \frac{\Delta(z/z_a)}{z_a}, \quad n(z) = n(z/z_a), \quad 0 < z_a \ll 1$$

where $\Delta = \Delta_1 < 0$, $n = 1$ inside the crystal; elsewhere $\Delta = \Delta_2 > 0$, $n = 0$ (linear). The analysis follows that in communications (see Chapter 10): we introduce multiple scales $\zeta = z/z_a$ (short), $Z = z$ (long), and expand the solution in powers of z_a : $u = u^{(0)} + z_a u^{(1)} + \dots$, $0 < z_a \ll 1$. At $O(1/z_a)$ we have a linear equation:

$$iu_\zeta^{(0)} + \frac{\Delta(\zeta)}{2} u_{\zeta\zeta}^{(0)} = 0,$$

which we solve via Fourier transforms in t and find, in the Fourier domain, that

$$\hat{u}^{(0)} = \hat{U}_0(Z, \omega) \exp \left[-i \frac{\omega^2}{2} C(\zeta) \right], \quad C(\zeta) = \int_0^\zeta \Delta(\zeta') d\zeta',$$

where $\hat{U}_0(Z, \omega)$ is free at this stage. Proceeding to the next order we find a forced linear equation. In order to remove unbounded growth, i.e., remove secularities, we find an equation for \hat{U}_0 that is given below:

$$i \frac{\partial \hat{U}_0}{\partial Z} - \frac{d_0}{2} \omega^2 \hat{U}_0 + \int_0^1 \exp \left[i \frac{\omega^2}{2} C(\zeta) \right] \left(\mathcal{F} \{ n(\zeta) |u^{(0)}|^2 u^{(0)} - R[u^{(0)}] \} \right) d\zeta = 0, \quad (11.3)$$

where \mathcal{F} represents the Fourier transform; i.e., $\mathcal{F} w(\omega) = \hat{w} = \int w(t) e^{-i\omega t} dt$. This equation is referred to here as the DM-PES equation or simply the averaged equation. The strength of the dispersion-management is usually measured by the map length, which we take in the normal and anomalous domains to be equal ($\theta = 1/2$ in the notation of Chapter 10) and so $s = |\Delta_1|/4$; we take the distance in the crystal to be the same as the distance in the prisms. The equation is a nonlinear integro-differential equation; as in the communications application it can be solved numerically. Similar to the constant dispersive case, for $d_0 > 0$ we find mode-locking. Fixing the parameters as $d_0 = E_0 = P_0 = 1$, $z_a = \tau = l = 0.1$ and varying the gain, we find that with sufficient gain strength mode-locking occurs. The mode-locking also depends on the strength of the dispersion-management: given a map strength, s , and where $g_* = g_*(s)$, we find: for $g < g_*$, pulses damp; for $g > g_*$, mode-locking. In Figure 11.7 is a typical example of the evolution of a unit Gaussian with map strength $s = 1$.

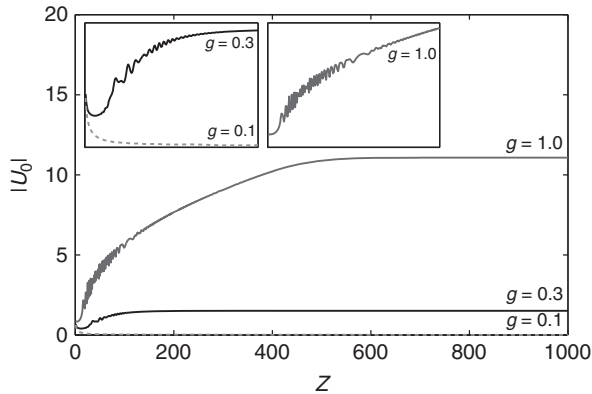


Figure 11.7 Evolution of the peak of a unit Gaussian using the DM-PES equation with $s = 1$ and gain parameters $g = 0.1$ (damped evolution), 0.3 and 1.0. In the inset, the early evolution of the peaks is shown.

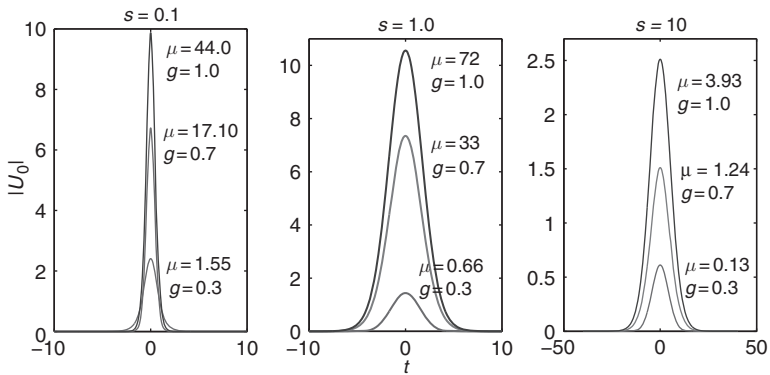


Figure 11.8 DM-PES solitons for various values of gain, g , and propagation constant, μ , with map strength $s = 1$.

The final mode-locking state corresponds to a soliton that can be obtained from spectral renormalization methods (discussed in Chapter 10). A soliton satisfies a fixed point integral equation obtained after substituting $\hat{U}_0(Z, \omega) \rightarrow \hat{U}_0(\omega)e^{i\mu Z}$ into the DM-PES equation (11.3). In Figure 11.8 are some typical solitons corresponding to different values of gain g and propagation constant μ . As in the constant dispersive case, DM-PES solitons correspond to specific values of μ , which is the soliton analog of mode-locking. This is also in contrast to the unperturbed case where solutions exist for all $\mu > 0$. We see that as map strength increases the solitons become smaller in amplitude but much more broad. As μ increases the modes become sharper and taller.

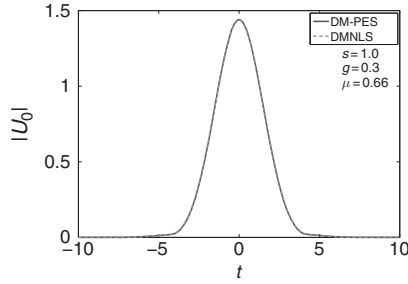


Figure 11.9 Typical comparison between the solutions of the DM-PES equation (11.3) and the pure DMNLS equation for $s = 1$ and $g = 0.3$.

Each mode-locked state is affected by strong saturation effects. Hence the soliton is essentially a solution of the unperturbed DM-PES equation (10.25) (where $g(\zeta)$ is replaced by $n(\zeta)$ in the notation of this section); i.e., this is the DMNLS equation that we obtain when we omit the gain and damping terms. This is indicated in Figure 11.9 for typical parameters. The main effect of the gain-damping is to isolate the parameters for which mode-locking occurs.

11.2.3 Remarks on perturbation theory

We have studied the behavior of both single solitons and soliton strings in ML lasers in detail via perturbation theory (Ablowitz et al., 2009a). Here we briefly mention some of the key results in the case of constant dispersion, taking $d_0 = 1$. Since the pulses have been found to be well approximated by solutions of classical NLS equation, we assume a soliton solution of the NLS form written as

$$u = ue^{i\phi}, \quad u = \eta \operatorname{sech}(\eta\theta), \quad \xi = \int_0^z V dz + t_0 \quad (11.4a)$$

$$\theta = t - \xi, \quad \sigma = \int_0^z \left[\mu + \frac{V^2}{2} \right] dz + \sigma_0, \quad \phi = V\theta + \sigma, \quad (11.4b)$$

with parameters for the height (η , $\mu = \eta^2/2$), velocity (V), temporal shift (t_0) and phase shift (σ_0) assumed to vary adiabatically, i.e., slowly, in z .

We consider the effects of gain, filtering and loss as perturbations of the NLS equation, taking $d_0 = n = 1$ in the PES equation,

$$iu_z + \frac{1}{2}u_{tt} + |u|^2 u = R[u] \quad (11.5)$$

where the right-hand side F contains the gain-damping terms and is assumed small. Recall

$$R = \frac{gu}{1 + E/E_0} + \frac{\tau u_{tt}}{1 + E/E_0} - \frac{lu}{1 + P/P_0}$$

and $E = \int_{-\infty}^{\infty} |u|^2 dt$, $P = |u|^2$. While the individual contributions of terms in F may not always be small, the combined effects are small; as discussed above they provide the mode-locking mechanism (Ablowitz and Horikis, 2008).

We find the equations for the evolution of the parameters η , V , t_0 , σ_0 by requiring the leading-order solution, (11.4), to satisfy a set of integrated quantities related to the (unperturbed) conservation laws suitably modified by the terms in $R[u]$. These can be derived directly from (11.5) as

$$\frac{d}{dz} \int |u|^2 = 2 \operatorname{Im} \int R[u] u^* \quad (11.6a)$$

$$\frac{d}{dz} \operatorname{Im} \int u u_t^* = 2 \operatorname{Re} \int R[u] u_t^* \quad (11.6b)$$

$$\frac{d}{dz} \int t |u|^2 = -\operatorname{Im} \int u u_t^* + 2 \operatorname{Im} \int t R[u] u^* \quad (11.6c)$$

$$\operatorname{Im} \int u_z u_\mu^* = -\frac{1}{2} \operatorname{Re} \int u_t u_\mu^* + \operatorname{Re} \int |u|^2 u u_\mu^* - \operatorname{Re} \int R[u] u_\mu^*, \quad (11.6d)$$

where all integrals are taken over $-\infty < t < \infty$.

When (11.4) are substituted into (11.6) the modified integral equations reduce to a system of differential equations that govern the evolution and mode-locking of soliton pulses:

$$\frac{d\eta}{dz} = g \left[\frac{2\eta}{2\eta + 1} \right] - \tau \frac{1}{2\eta + 1} \left[\frac{2}{3} \eta^3 + 2V^2 \eta \right] + l \left[2\eta \frac{1}{a-b} \log \left(\frac{a}{b} \right) \right] \quad (11.7a)$$

$$\frac{dV}{dz} = -\tau V \left[\frac{4}{3} \frac{\eta^2}{2\eta + 1} \right] \quad (11.7b)$$

$$\frac{dt_0}{dz} = 0 \quad (11.7c)$$

$$\frac{d\sigma_0}{dz} = 0; \quad (11.7d)$$

here a and b are the roots of the polynomial $x^2 + 2(1 + 2\eta^2)x + 1 = 0$ (we can choose a and b to be either root). Note, the first two equations are independent of t_0 and σ_0 , both of which are constant. We only consider parameters in the domain $\eta \geq 0$ (since $\eta < 0$ can be represented as a positive η with a π phase shift).

Consider the case $V = 0$; this is the only equilibrium for V and it is stable for $\eta > 0$. In this case we find an equation for η independent of any other parameters

$$\frac{d\eta}{dz} = g \left[\frac{2\eta}{2\eta + 1} \right] - \tau \frac{1}{2\eta + 1} \left[\frac{2}{3}\eta^3 \right] + l \left[2\eta \frac{1}{a-b} \log \left(\frac{a}{b} \right) \right],$$

which accurately predicts the mode-locking behavior found numerically. Clearly, η has at least one equilibrium at 0, which can be proved to be stable for $g < l$ and unstable for $g > l$. For $g > l$ there is a second equilibrium that is stable and corresponds to the mode-locked solution, as indicated in Figure 11.10.

Weakly interacting solitons can also be studied analytically by considering the interaction terms as a small perturbation (Karpman and Solov'ev, 1981). We refer the interested reader to Ablowitz et al. (2009a) for further details.

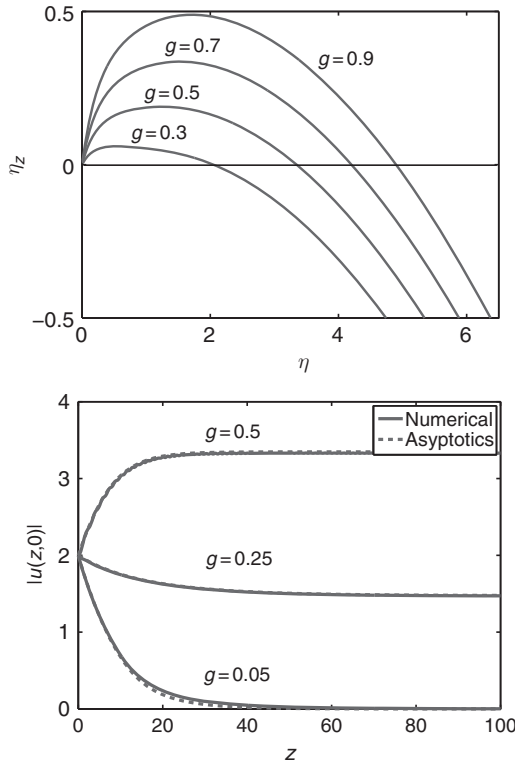


Figure 11.10 Phase portrait of the amplitude equation for several values of $g > l$ illustrating the single stable equilibrium (top). Comparison of asymptotic and numerical results for mode-locking pulses (bottom).

11.2.4 The normal regime

The dynamics of pulses evolving under the PES equation in the normal regime ($d_0 < 0$) are studied next. As above, all terms are kept constant and only the gain parameter g is changed. Typical values are taken: $d_0 = -1$ (i.e., the normal regime), $n = 1$, $E_0 = P_0 = 1$, $\tau = l = 0.1$. We study the evolution of an initial unit Gaussian pulse peak for different values of the gain parameter g ; see Figure 11.11. When $g = 0.1$ the pulse decays quickly due to excessive loss with no noticeable oscillatory or chaotic behavior; the pulse exhibits damped evolution. When $g = 0.5$, due to the loss in the system the pulse undergoes an initial decrease and then very slowly dissipates. When $g = 1.5$ a localized evolution is obtained. With sufficient gain in the system, the pulse amplitude initially

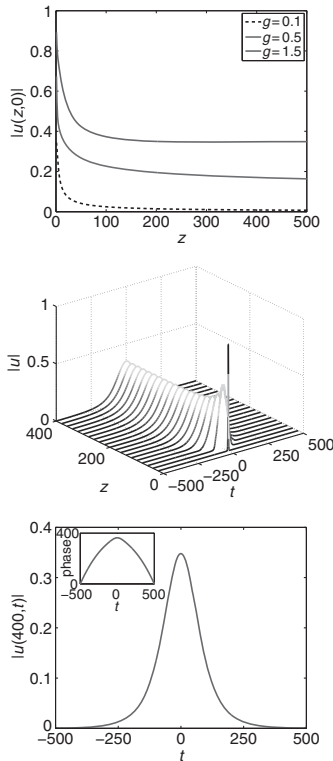


Figure 11.11 Evolution of the pulse peak of an initial profile under the PES equation, in the normal regime ($d_0 = -1$) with different values of gain. Top: the damped pulse-peak evolution is shown with a dashed line. Middle: the complete evolution is given for $g = 1.5$. Bottom: the resulting soliton and the corresponding phase in the inset.

decreases but then a steady state is reached. The sharp and narrow initial Gaussian rapidly evolves into a wide but finite-energy pulse. Three regimes are observed: (a) when the loss is much greater than the gain the pulse decays to zero; (b) when the loss is again a prominent effect but sufficient gain exists in the system to sustain a very slowly decaying evolution resulting in a “quasi-soliton” state; and (c) the soliton regime above a certain value of gain. When a localized state results in the normal regime, there is a strong phase effect, as indicated in Figure 11.11. This is unlike the anomalous regime where the pulse’s temporal phase is constant and the pulses have relatively much narrower width.

As indicated above, the values for the gain, loss and filtering parameters provide operating regions of the laser system that depend critically on the gain parameter. The parameters d_0 , E_0 , P_0 , g , τ , l were chosen to have typical values. Changing these values to more closely correspond to experimental data shows that the above observations are quite general (see Ablowitz and Horikis, 2008, 2009b).

Bi-solitons

As mentioned above, individual pulses of (11.2) in the normal regime exhibit strong chirp and cannot be identified as the solutions of the “unperturbed” NLS equation. Indeed, the classical NLS equation does not exhibit decaying “bright” soliton solutions in the normal regime. If we begin with an initial Gaussian, $u(0, t) = \exp(-t^2)$, the evolution of the PES equation mode-locks into a fundamental soliton state. On the other hand, we can obtain a higher-order antisymmetric soliton, i.e., an antisymmetric bi-soliton, one that has its peak amplitudes differing in phase by π . Such a state can be obtained if we start with an initial state of the form $u(0, t) = t \exp(-t^2)$ (i.e., a Gauss–Hermite polynomial). The evolution results in an antisymmetric bi-soliton and is shown in Figure 11.12 along with a comparison to the profile of the single soliton. This is a true bound state. Furthermore, the results of our study finding antisymmetric solitons in the normal regime are consistent with experimental observations (Chong et al., 2008a).

It is interesting that the normal regime also exhibits higher soliton states when two general initial pulses (e.g., unit Gaussians) are taken sufficiently far apart. The resulting pulses, shown in Figure 11.13, individually have a similar shape to the single soliton of the normal regime with lower individual energies. These pulses if initially far enough apart can have independent chirps that may be out of phase by an arbitrary constant. We again find that the minimum distance required for the two solitons to remain apart is $d^* \approx 9\alpha$ which is a good estimate for the required pulse separation just as in the constant anomalous dispersive case! These pulses are “effective bound states” in that after a long

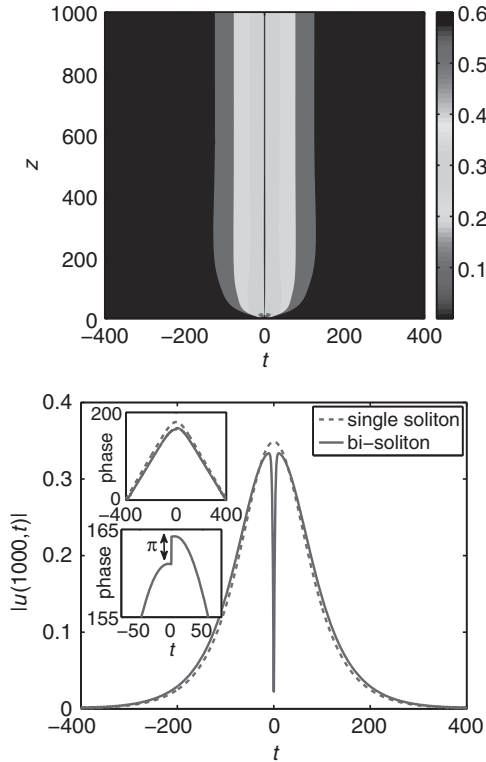


Figure 11.12 Evolution of the antisymmetric soliton (top) and the antisymmetric bi-soliton, in the normally dispersive regime, superimposed with the corresponding single soliton (bottom) at $z = 1000$. Here $g = 1.5$.

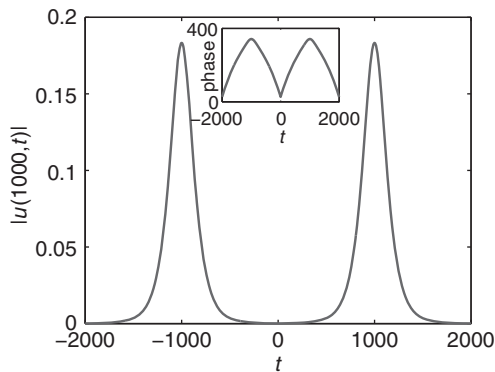


Figure 11.13 Symmetric two-soliton state of the normal regime with in-phase pulses. The phase structure is depicted in the inset. Here $g = 1.5$.

distance they separate very slowly. Additional higher-order 3-, 4-, ... soliton states can also be found. We refer the reader to Ablowitz et al. (2009c) for further details.

Asymptotic approximations of normal solitons

Using the spectral renormalization method, we have found localized pulses in the normal dispersive regime for a broad range of parameters, provided that sufficient gain is present in the system. These pulses are slowly varying in t , with a large phase. This suggests that by assuming a slow time-scale in the equation and using perturbation theory (i.e., a WKB-type expansion) the soliton system can be reduced to simpler ordinary differential equations for the amplitude and the phase of the pulse. The first step before performing perturbation theory is to write the solution of (11.2) in the form $u(z, t) = R \exp(i\mu z + i\theta)$, where $R = R(t)$ and $\theta = \theta(t)$ are the pulse amplitude and phase, respectively. Substituting into the equation and equating real and imaginary parts and calling $\epsilon = 1/E_0$, $\delta = 1/P_0$, we get

$$-\mu R - \frac{d_0}{2} (R_{tt} - R\theta_t^2) + R^3 = -\frac{\tau}{1 + \epsilon E} (2R_t\theta_t + R\theta_{tt}) \quad (11.8a)$$

$$-\frac{d_0}{2} (2R_t\theta_t + R\theta_{tt}) = \frac{g}{1 + \epsilon E} R + \frac{\tau}{1 + \epsilon E} - \frac{l}{1 + \delta R^2} R. \quad (11.8b)$$

We then take the characteristic time length of the pulse to be such that we can define a scaling in the independent variable of the form $\nu = T/t$ or $T = \nu t$ so that $R = R(\nu t)$, $\theta_t = O(1)$ (i.e., θ is large) and $\theta_{tt} = O(\nu)$ where $\nu \ll 1$. Then (11.8a) becomes

$$-\mu R + \frac{d_0}{2} R\theta_t^2 + R^3 = \frac{d_0}{2} \nu^2 R_{TT} - \frac{\tau}{1 + \epsilon E} (2\nu R_T\theta_t + R\theta_{tt}).$$

The leading-order equation is

$$\theta_t^2 = \frac{2}{d_0} (\mu - R^2). \quad (11.9)$$

Using the same argument and this newly derived equation (11.9) we then find that (11.8b) to leading order reads

$$R_t = -\operatorname{sgn}(t) \frac{\sqrt{2(\mu - R^2)/d_0}}{3R^2 - 2\mu} \left(\frac{g}{1 + \epsilon E} - \frac{4\tau(\mu - R^2)/d_0}{1 + \epsilon E} - \frac{l}{1 + \delta R^2} \right). \quad (11.10)$$

This is now a non-local first-order differential equation for $R = R(t)$, since $E = \int_{-\infty}^{\infty} R^2 dt$. From the above equation (11.9), imposing $\theta_t(t = 0) = 0$, it follows that $\mu \approx R^2(0)$.

To remove the non-locality another condition is needed and it is based on the singular points of (11.10). Recall that $R(t)$ is a decaying function in $t \in [0, +\infty)$

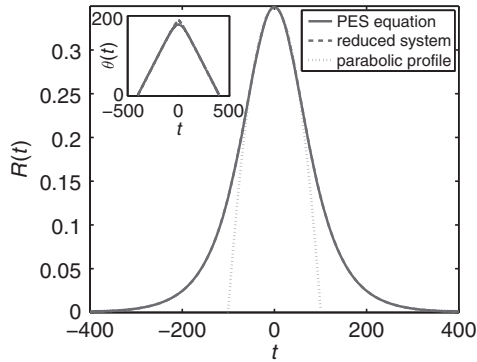


Figure 11.14 Solutions of the complete PES equation and the reduced system, in the normally dispersive regime. The relative parabolic profile is also shown. Here $g = 1.5$.

and $\mu \approx R^2(0) \geq R(t)^2$. Thus there exists a point in t such that the denominator in the equation becomes zero. To remove the singularity we require that the numerator of the equation is also zero at the same point; that leads to

$$1 + \epsilon E = \frac{1}{l} \left(g - \frac{2\tau}{3d_0} \mu \right) \left(1 + \frac{2\delta}{3} \mu \right).$$

Thus (11.10) is now a first-order equation that can be solved by standard numerical methods and analyzed by phase plane methods. The resulting solutions from the PES equation and the reduced equations are compared in Figure 11.14. Notice that here $\mu = 0.1216$ while $R^2(0) = 0.1218$.